

Available online at [www.sciencedirect.com](http://www.sciencedirect.com)

ScienceDirect

Journal homepage: [www.elsevier.com/locate/cortex](http://www.elsevier.com/locate/cortex)

## Research Report

# Structural organization of the praxis network predicts gesture production: Evidence from healthy subjects and patients with schizophrenia



Petra V. Viher <sup>a,b,\*</sup>, Ahmed Abdulkadir <sup>c</sup>, Peter Savadijev <sup>b,d,e</sup>, Katharina Stegmayer <sup>a</sup>, Marek Kubicki <sup>b,d,f</sup>, Nikos Makris <sup>b,g</sup>, Sarina Karmacharya <sup>b</sup>, Andrea Federspiel <sup>a</sup>, Stephan Bohlhalter <sup>h,i</sup>, Tim Vanbellingen <sup>h,i,j</sup>, René Müri <sup>h,k</sup>, Roland Wiest <sup>l</sup>, Werner Strik <sup>a</sup> and Sebastian Walther <sup>a</sup>

<sup>a</sup> Translational Research Center, University Hospital of Psychiatry and Psychotherapy, University of Bern, Bern, Switzerland

<sup>b</sup> Psychiatry Neuroimaging Laboratory, Department of Psychiatry, Brigham and Women's Hospital, Harvard Medical School, Boston, USA

<sup>c</sup> University Hospital of Old Age Psychiatry and Psychotherapy, University of Bern, Bern, Switzerland

<sup>d</sup> Department of Radiology, Brigham and Women's Hospital, Harvard Medical School, Boston, USA

<sup>e</sup> Department of Diagnostic Radiology, McGill University, Montreal, Canada

<sup>f</sup> Department of Psychiatry, Massachusetts General Hospital, Harvard Medical School, Boston, USA

<sup>g</sup> Departments of Psychiatry, Neurology and Radiology, Athinoula A. Martinos Center for Biomedical Imaging, Massachusetts General Hospital, Harvard Medical School, Boston, USA

<sup>h</sup> Department of Clinical Research, University Hospital, Inselspital, Bern, Switzerland

<sup>i</sup> Neurocenter, Luzerner Kantonsspital, Lucerne, Switzerland

<sup>j</sup> Gerontechnology and Rehabilitation Group, University of Bern, Bern, Switzerland

<sup>k</sup> Department of Neurology, University Hospital Inselspital, University of Bern, Bern, Switzerland

<sup>l</sup> Support Center of Advanced Neuroimaging, Institute of Neuroradiology, University of Bern, Bern, Switzerland

## ARTICLE INFO

## Article history:

Received 13 September 2019

Reviewed 13 January 2020

Revised 11 April 2020

Accepted 19 May 2020

Action editor Gereon Fink

Published online 27 August 2020

## Keywords:

Diffusion weighted MRI

Gesture

## ABSTRACT

Hand gestures are an integral part of social interactions and communication. Several imaging studies in healthy subjects and lesion studies in patients with apraxia suggest the praxis network for gesture production, involving mainly left inferior frontal, posterior parietal and temporal regions. However, little is known about the structural connectivity underlying gesture production. We recruited 41 healthy participants and 39 patients with schizophrenia. All participants performed a gesture production test, the Test of Upper Limb Apraxia, and underwent diffusion tensor imaging. We hypothesized that gesture production is associated with structural network connectivity as well as with tract integrity. We defined the praxis network as an undirected graph comprised of 13 bilateral regions of interest and derived measures of local and global structural connectivity and tract integrity from Finsler geometry. We found an association of gesture deficit with reduced global and

\* Corresponding author. University Hospital of Psychiatry and Psychotherapy, Bolligenstrasse 111, 3000 Bern 60, Switzerland.

E-mail address: [petra.viher@upd.unibe.ch](mailto:petra.viher@upd.unibe.ch) (P.V. Viher).

<https://doi.org/10.1016/j.cortex.2020.05.023>

0010-9452/© 2020 The Author(s). Published by Elsevier Ltd. This is an open access article under the CC BY license (<http://creativecommons.org/licenses/by/4.0/>).

Nonverbal communication  
Structural connectivity

local efficiency of the praxis network. Furthermore, reduced tract integrity, for example in the superior longitudinal fascicle, arcuate fascicle or corpus callosum were related to gesture deficits. Our findings contribute to the understanding of structural correlates of gesture production as they first present diffusion tensor imaging data in a combined sample of healthy subjects and a patient cohort with gestural deficits.

© 2020 The Author(s). Published by Elsevier Ltd. This is an open access article under the CC BY license (<http://creativecommons.org/licenses/by/4.0/>).

## 1. Introduction

Gestures play an important role in language and communication. They support language production and comprehension, and are critically involved in nonverbal communication as they transmit information independent from language (Goldin-Meadow & Alibali, 2013). Gestures are not only coupled to language, but are also strongly related to the motor domain, and can be interpreted as body movements that support the cognitive system (Pouw et al., 2014).

As behavioral output of complex language–motor interactions, gestures require the interplay and coordination of various brain regions. For instance, tool use depends on a left-lateralized network that includes a dorsal stream for object localization and a ventral stream for object recognition (Ramayya et al., 2010). Furthermore, the dorsal pathway can be divided into a dorso-dorsal and a ventro-dorsal pathway (Binkofski & Buxbaum, 2013). The dorso-dorsal pathway forms the grasp system and processes structural characteristics of objects, which is necessary for the production of actions. While the ventro-dorsal stream, termed the use system, is responsible for the long-term storage of skilled tool use actions (Binkofski & Buxbaum, 2013). Thus, tool use involves several temporal and parietal regions including the middle temporal gyrus (MTG), which stores semantic and conceptual information of tools, the posterior supramarginal gyrus (SMG) and angular gyrus (AG), which store representations of invariant features of meaningful gestures, and the anterior SMG, which is important for the planning of gestures and generation of a motor plan (Ramayya et al., 2010). Finally, also the ventral premotor cortex and the inferior frontal gyrus (IFG), which store motor programs for grasping and manipulation of objects are involved (Ramayya et al., 2010).

A number of functional magnetic resonance imaging (fMRI) studies in healthy subjects explored brain activity during planning or execution of gestures. Planning, pantomime, and execution of tool use gestures share the involvement of several regions, including the inferior parietal lobe (IPL), superior parietal lobe (SPL), MTG, superior temporal gyrus (STG), premotor cortex and IFG (Hermsdorfer et al., 2007; Johnson-Frey et al., 2005). Similar regions are engaged during the planning of communicative gestures, for example the intraparietal sulcus (IPS), the SMG, the SPL and premotor areas (Bohlhalter et al., 2009; Kroliczak & Frey, 2009). Nevertheless, more complex and cognitively demanding gestures may require the recruitment of additional brain regions. For example, pantomime of tool use

activates additional brain areas compared to imitation of meaningless gestures, such as the pars triangularis of the IFG, the MTG, the SMG and the IPS (Vry et al., 2015). Taken together, the planning and execution of gestures activate the praxis network that includes distinct posterior parietal, inferior frontal and temporal brain regions (Bohlhalter et al., 2009; Hermsdorfer et al., 2013; Johnson-Frey et al., 2005; Kroliczak & Frey, 2009).

The importance of posterior parietal areas and its connectivity to motor areas for gesture production is known from early lesion studies in patients with apraxia following left hemispheric brain damage. Apraxia is conceptualized as dysconnectivity between motor and speech areas (Geschwind, 1965). Patients with apraxia present deficits in the imitation of gestures, pantomime of gestures and actual tool use (Goldenberg & Hagmann, 1998). Tool use in patients with apraxia depends on the MFG, the IFG and posterior parietal regions, such as the IPL (including SMG and AG) (Goldenberg, 2009; Goldenberg & Spatt, 2009; Haaland et al., 2000; Randerath et al., 2010). Pantomime of tool use has been related to the posterior middle and inferior temporal lobe and adjacent regions of the occipital lobe (Buxbaum et al., 2014). Additionally, pantomime involves the IFG, precentral gyrus, premotor area (Goldenberg et al., 2007; Weiss et al., 2016), IPL, IPS and SPL (Hoeren et al., 2014). Imitation of meaningful gestures depends on the IFG, premotor cortex, precentral regions and MTG, whereas imitation of meaningless gestures includes predominantly central areas and small parts of the pars triangularis of the IFG (Weiss et al., 2016). In addition, a contribution of the posterior parietal lobe is suggested, with the AG more critically related to the imitation of meaningless gestures and the SMG more involved in meaningful gestures (Mengotti et al., 2013). Taken together, similar to fMRI studies including healthy subjects, lesion mapping in apraxia identified a common network for pantomime and imitation of gestures, which comprises the IFG, posterior temporal, inferior parietal and motor areas (Buxbaum et al., 2014; Weiss et al., 2016).

However, little is known about the structural pathways connecting important components of the praxis network. In healthy subjects, four pathways have been identified in tool use that connect the MTG, the anterior and posterior SMG and the frontal lobe (Ramayya et al., 2010). The functional role of the pathways includes the integration of non-spatial and semantic information into a gesture plan and the transformation of this plan into a physical action (Ramayya et al., 2010). Pantomime of tool use depends on the dorsal stream, including the superior longitudinal fascicle (SLF) II and the arcuate fascicle (AF), and fibers connecting the pars triangularis of the IFG with the MTG

and the IPL (Vry et al., 2015). In contrast, imitation of meaningless gestures involves only the dorsal stream for sensory-motor conversion (Vry et al., 2015).

On the one hand, healthy subjects demonstrate intact white matter (WM) organization and gesture production and hence do not inform about the neural underpinnings of gesture deficits. On the other hand, patients with severe gesture deficits, such as patients with apraxia, present macroanatomical brain lesions that hamper investigations using diffusion tensor imaging (DTI). We included patients with schizophrenia, a disorder that is characterized by both, widespread WM alterations and considerable impairments in gesture production. WM abnormalities in schizophrenia have been reported in several fiber tracts, including the corpus callosum, the SLF, the inferior longitudinal fascicle, the AF and the uncinate fascicle (UF) (Whitford et al., 2011). Patients with schizophrenia also show reduced connectivity of central brain regions as reflected by rich club organization of the structural network (van den Heuvel et al., 2013). In addition, schizophrenia patients present gesture deficits at multiple levels: they use gestures less frequently (Lavelle et al., 2013), incongruent to their speech (Millman et al., 2014) and display impairments in the production of hand gestures (Walther et al., 2013, 2015).

Consequently, patients with schizophrenia, in contrast to patients with macroscopic lesions, show only microstructural WM alterations, but also behavioral gesture deficits. Studying the gesture deficit in relationship with WM changes in schizophrenia may therefore aid understanding the neural basis of gesture production. Thus, the aim of this study was to investigate whether structural network connectivity and tract integrity are correlated with gesture production in healthy subjects and schizophrenia patients.

The praxis network was modeled as a graph. We describe the nodes of the graph (brain regions) of an anatomical atlas. We defined the connecting edges as structural connectivity between pairs of nodes that derived from tractographic measures, similar to the notions in functional connectivity (Bullmore & Sporns, 2009). We then derived metrics from the connectivity structure. Global network efficiency is inversely related to path length. The path length describes the minimum number of edges that have to be passed in order to get from one node to another (Bullmore & Sporns, 2009). Thus, complex networks have short path lengths and high global efficiency of information transfer (Bullmore & Sporns, 2009). The global efficiency is maximal for a fully connected network and minimal for a fully disconnected network (Sporns, 2013). Furthermore, local efficiency of a node describes how efficient its immediate neighbors communicate when the node itself is removed (Latora & Marchiori, 2001).

We hypothesized that gesture impairments in healthy subjects and schizophrenia patients correlate with lower local and global efficiency of the praxis network. Especially the local efficiency of key regions, such as the IFG, IPL, STG and MTG are expected to strongly predict gesture production. Furthermore, specific connections of the praxis network are assumed to predict gesture production across groups. These include inter-hemispheric connections between the IFG and IPL, intrahemispheric fronto-parietal and fronto-temporal connections as well as important tracts of the praxis network, e.g., the UF, AF or SLF III.

## 2. Methods

### 2.1. Participants

In this section, we report how we determined our sample size, all data exclusions, all inclusion/exclusion criteria, whether inclusion/exclusion criteria were established prior to data analysis, all manipulations, and all measures in the study. The analyses codes are provided online (<https://github.com/AbdulkadirA/praxis-network-gestures>). Thirty-nine patients with schizophrenia (77%), schizophreniform (18%) or schizoaffective disorders (5%) and 41 matched healthy controls participated in this study. All patients were recruited from the inpatient and outpatient departments of the University Hospital of Psychiatry and Psychotherapy Bern, Switzerland, and all controls among staff and via advertisement. Patients and controls were matched for age, sex and education (Table 1). All participants were right-handed according to the Edinburgh Handedness Inventory (Oldfield, 1971). We calculated the power analysis with G\*Power 3.1 (Faul et al., 2007, 2009) for differences between two independent groups (effect size = .8,  $\alpha$  = .05, power = .95) resulting in a sample size of 42 subjects per group. After the exclusion of 8 subjects due to bad image quality, 80 participants remained in the final sample size.

The study was approved by the local ethics committee (KEK-BE 025/13) and conducted in accordance with the Declaration of Helsinki. Informed consent was obtained from all subjects and the capacity of the patients to give informed consent was confirmed by their treating psychiatrist. No part of the study procedure and analyses was pre-registered prior to the research being conducted. The conditions of our ethics approval do not permit sharing of the data supporting this study with any individual outside the author team under any circumstances.

Patients were diagnosed with schizophrenia, schizoaffective or schizophreniform disorders according to the Diagnostic and Statistical Manual of Mental Disorders, fifth edition, in short DSM-5. Additional assessments included the Mini International Neuropsychiatric Interview (MINI)

**Table 1 – Demographic and clinical characteristics.**

Variables <sup>a</sup>	Controls (n = 41)	Patients (n = 39)	Statistics		
			X <sup>2</sup>	df	p
Sex (men/ women)	23/18	24/15	.244	1	.621
	Mean (SD)	Mean (SD)	t	df	p
Age (years)	38.93 (13.69)	38.08 (11.21)	-.303	78	.763
Education (years)	14.20 (2.73)	13.63 (3.23)	-.850	78	.398
TULIA total score	225.86 (7.86)	210.31 (17.50)	-5.171	78	.001
CPZ (mg) 5 years		221.19 (285.84)			
DOI (months)		137.77 (144.32)			
PANSS positive		17.82 (6.04)			
PANSS negative		17.64 (4.51)			
PANSS total		70.44 (17.47)			

<sup>a</sup> CPZ, average chlorpromazine equivalents for the last five years; DOI, duration of illness; PANSS, positive and negative syndrome scale.

(Sheehan et al., 1998), the Comprehensive Assessment of Symptoms and History (Andreasen et al., 1992) and the Positive and Negative Syndrome Scale (PANSS) (Kay et al., 1987). The majority of the patients (90%) received antipsychotic medication. Dosages were calculated as the average chlorpromazine equivalents (CPZ) per day (Woods, 2003) for the past five years. Demographic and clinical characteristics of all participants are given in Table 1.

Our sample did not include patients that had any substance abuse or dependencies other than nicotine, past or current medical or neurological conditions associated with either movement impairments or WM abnormalities (e.g., stroke, multiple sclerosis), and histories of either head trauma with loss of consciousness or electroconvulsive treatment. Healthy controls had no history of any psychiatric disorder as well as no first-degree relatives with schizophrenia spectrum disorders. Participants had no contraindications to magnetic resonance imaging (MRI) scans (e.g., metallic implants, pregnancy and claustrophobia).

## 2.2. Behavioral assessment

Production of gestures was assessed using the Test of Upper Limb Apraxia (TULLA) (Vanbellingen et al., 2010), which has also been validated in schizophrenia (Walther et al., 2013). Performance of 48 items was videotaped and later evaluated by a rater blind to diagnoses. Potential errors can be attributed to temporal–spatial features or to the content. The score ranges from 0 to 240, whereby a higher score indicates a superior performance. Further, performance was tested in two different domains: in an imitation domain (performance after demonstration by the examiner) and in a pantomime domain (performance after verbal instruction). In addition, both domains include three semantic categories: meaningless (e.g., put your index finger on the tip of your nose), intransitive (e.g., wave goodbye), and transitive gestures (e.g., use a hammer).

## 2.3. MRI acquisition

All subjects were scanned on a 3T MRI scanner (Siemens Magnetom Trio; Siemens Medical Solutions, Erlangen, Germany) with a 12-channel radio frequency headcoil. We obtained a T1-weighted MDEFT (modified driven equilibrium Fourier transform pulse) sequence (Deichmann et al., 2004) for anatomical brain imaging (176 sagittal slices,  $1 \times 1 \times 1 \text{ mm}^3$ , matrix size  $256 \times 256$ ), with a field of view (FOV) of  $256 \times 256 \text{ mm}^2$ , 7,92 msec repetition time (TR), 2,48 msec echo time (TE), 910 msec inversion time (TI) and a flip angle (FA) of  $16^\circ$ . The acquisition time was 13 min.

For DTI acquisition, we used a spin echo planar imaging sequence (59 slices, FOV =  $256 \times 256 \text{ mm}^2$ , sampled on a  $128 \times 128$  matrix, slice thickness = 2 mm, gap between slices = 0 mm, resulting in  $2 \text{ mm}^3$  isotropic voxel resolution) and TR/TE = 8000/92 msec covering the whole brain (40 mT/m gradient, 6/8 partial Fourier, acceleration factor 2, bandwidth 1346 Hz/pixel). Diffusion-weighted images (DWI) were set in the axial plane parallel to the AC-PC line and measured along 42 directions applying a  $b$ -value =  $1300 \text{ sec/mm}^2$ . In order to generate the DTI data, a balanced and rotationally invariant

diffusion-encoding scheme was applied over the unit sphere. Acquisition time lasted 6 min.

## 2.4. Data processing

We used a publically available in-house pipeline (<https://github.com/pnlbwh/pnlutil>, commit 4c6cd73) to process the data. The T1 and diffusion weighted images were transformed from DICOM to NRRD file format. The images were then automatically aligned to the AC-PC axis and centered. All scans were visually controlled for image quality and orientation. Then, the analysis pipeline was separated into two processing streams (GM and WM).

### 2.4.1. Grey matter processing stream

All non-brain areas were excluded using a brain masking technique that is based on multi-atlas brain segmentation (Del Re et al., 2016). This technique has shown to be more accurate than the brain masks that are generated by FreeSurfer (Del Re et al., 2016). The masked images were then processed using FreeSurfer version 5.3. (Athinoula A. Martinos Center for Biomedical Imaging, Charlestown, Massachusetts, USA) in order to obtain a cortical parcellation and subcortical segmentation. A detailed description of the pipeline has been provided in previous publications (Dale et al., 1999; Fischl, 2012; Fischl et al., 1999) and is available on the FreeSurfer website (<http://ftp.nmr.mgh.harvard.edu/fswiki/recon-all>). The FreeSurfer parcellation was visually quality-controlled for each subject and slice.

### 2.4.2. White matter processing stream

First, we corrected the DWI volumes for affine distortions caused by eddy currents or due to head motion using an internal software. Tensor masks were created to exclude non-brain areas using the 3D Slicer software package version 4.5 ([www.slicer.org](http://www.slicer.org)) and were subsequently edited manually. Whole-brain two-tensor tractography was then performed for each subject (Malcolm et al., 2010). Finally, the FreeSurfer white matter was non-linearly subject-wise registered to the diffusion space.

### 2.4.3. Structural network connectivity

Structural connectivity analysis was performed using Finsler geometry (Dela Haije et al., 2019). In short, we computed an  $86 \times 86$  connectivity matrix based on the path measures for each subject that comprises the connectivity values between all neocortical regions of the default atlas in FreeSurfer (Desikan-Killiany atlas; (Desikan et al., 2006)). Local and global efficiency measures were computed based on each subject's connectivity matrix, using the Brain Connectivity Toolbox implementation (Rubinov & Sporns, 2010), and edge-level analyses were calculated in Matlab version 2017a. The full undirected connectivity graph thus comprised  $n = 86$  nodes and  $\binom{n}{2} = \frac{n!}{(n-k)!k!} = 3655$  edges. A subset of 13 out of 86 regions was chosen to represent the praxis network, which was used for further analyses. The selected frontal ROIs included the pars opercularis, orbitalis, and triangularis of the IFG, the precentral gyrus and the insula. The parietal ROIs comprised the SPL and IPL (including a separate ROI for the SMG). Finally, the temporal ROIs were the transverse temporal lobe, the STG, the banks of STS, the



parahippocampal gyrus and the MTG. Global and local connectivity was calculated based on the 13 bilateral ROIs.

#### 2.4.4. Structural integrity of selected connections/tracts

In addition to the structural network connectivity metrics, we were also interested in some specific tracts (see Table 3) based on the literature. We used WM query language (Wassermann et al., 2016) to determine for each tract the inter-ROI edges involved. Two of the connections were part of the corpus callosum, one connecting the bilateral IFG and the other connecting the bilateral IPL. The other six bilateral connections were the ones between the IFG and the IPL, between the frontal and the temporal areas, between the frontal and the parietal areas, the UF, AF and SLF III. The connections between the frontal and parietal areas, as well as frontal and temporal areas, were based on the findings of the literature (Duffau et al., 2005; Makris & Pandya, 2009; Vry et al., 2015). We also defined the other tracts according to the literature, the UF (Catani et al., 2002; Petrides & Pandya, 1988), AF (Duffau et al., 2008; Makris et al., 2005; Petrides & Pandya, 1988; Rilling et al., 2008) and SLF III (Makris et al., 2005). The definitions of the connections can be found in the supplementary material.

### 2.5. Statistical analysis

All statistical analyses were performed using IBM SPSS version 24 or Matlab version 2017a. Demographic and clinical data were compared using a chi-square test or independent t-tests in SPSS where appropriate. We used linear regression analyses to test whether structural network connectivity and structural integrity of selected connections and tracts (predictor variables) had an effect on the behavioral gesture performance (response variable). In detail, predictor variables were individual measures of integrity (one per tract), local efficiency (one per node), or global efficiency (one per subject). The response variable was either global gesture production, or the two TULIA domains separately (pantomime or imitation). Age, sex, and total intracranial volume (TIV) were included as covariates of no interest into our analyses. Furthermore, in an analysis of covariance (ANCOVA) with the same covariates, we examined if the global and local efficiency and specific connections of the praxis network were different between patients with schizophrenia and controls. The results of all linear models were corrected for multiple comparisons using the false discovery rate (FDR) threshold of  $p < .05$  (Nichols & Hayasaka, 2003).

## 3. Results

### 3.1. Behavioral and clinical data

Demographic and clinical characteristics of the subjects are given in Table 1. Patients with schizophrenia and healthy controls did not differ regarding sex, age, or education ( $p > .05$ ). As expected, the groups differed in the TULIA scores, indicating inferior gesture performance in schizophrenia.

### 3.2. Group differences in structural brain connectivity

Group differences in the structural connectivity were explored using an ANCOVA (see Table S5 in the supplementary material).

The means of both global efficiency and local efficiency of all ROIs except the bilateral SPL, right precentral gyrus and right parahippocampal gyrus differed significantly between groups ( $p < .05$ , FDR corrected). In addition, the connectivity between the left and right IFG, the bilateral UF and left AF differed between groups ( $p < .05$ , FDR corrected), indicating that patients displayed lower connectivity values than controls.

### 3.3. Associations of structural brain connectivity and gesture production

The linear regression analyses revealed that gesture production across groups is predicted by global and local efficiency, and by structural integrity of specific connections/tracts (see Figs. 1 and 2, Tables 2 and 3). Gesture production is related to both hemispheres; however, the left hemisphere seems to play a slightly more important role. In detail, global efficiency of the praxis network is significantly associated with gesture production across all subjects, and also separately within the group of patients, but not within controls (see Table 2). Local efficiency of all ROIs within the praxis network, except the right parahippocampal gyrus, predicted gesture production across groups, but not in each group separately. In addition to local and global efficiency, we were also interested whether structural integrity of selected connections or tracts within the praxis network would predict gesture production. All of our connections and tracts of interest, except the left fronto-temporal connection, were associated with gesture production across groups. The associations within each group separately were again not significant (see Table 3).

Supplementary video related to this article can be found at <https://doi.org/10.1016/j.cortex.2020.05.023>

In additional analyses, we were interested whether there are differences in the two domains of the TULIA, pantomime and imitation (see Figs. 3 and 4). Pantomime performance was significantly associated with global efficiency and local efficiency of all ROIs, excluding the right SPL and STG (see Table S1) across groups, but not in each group separately. Likewise, all connections of interest predicted pantomime performance across groups, except for the left fronto-temporal connection, but again not in each group alone (see Table S2).

A slightly different picture appears for imitation. Global efficiency predicted imitation performance across groups and in patients, but not in controls (see Table S3). Local efficiency of all ROIs, with the exception of the right parahippocampal gyrus, predicted imitation performance across groups and local efficiency of some of the ROIs predicted further imitation performance in the group of patients (see Table S3). In addition, some connections of interest correlated with imitation performance across groups, but not in each group alone (see Table S4).

Finally, we were interested in the edge-level connections between all ROIs. We detected many significant connections between frontal, parietal and temporal key areas of the praxis network ( $p < .05$ , FDR corrected). These results are partly depicted in Figs. 1, 3 and 4 and completely in Figures S1–S3 in the supplementary material.

Supplementary video related to this article can be found at <https://doi.org/10.1016/j.cortex.2020.05.023>

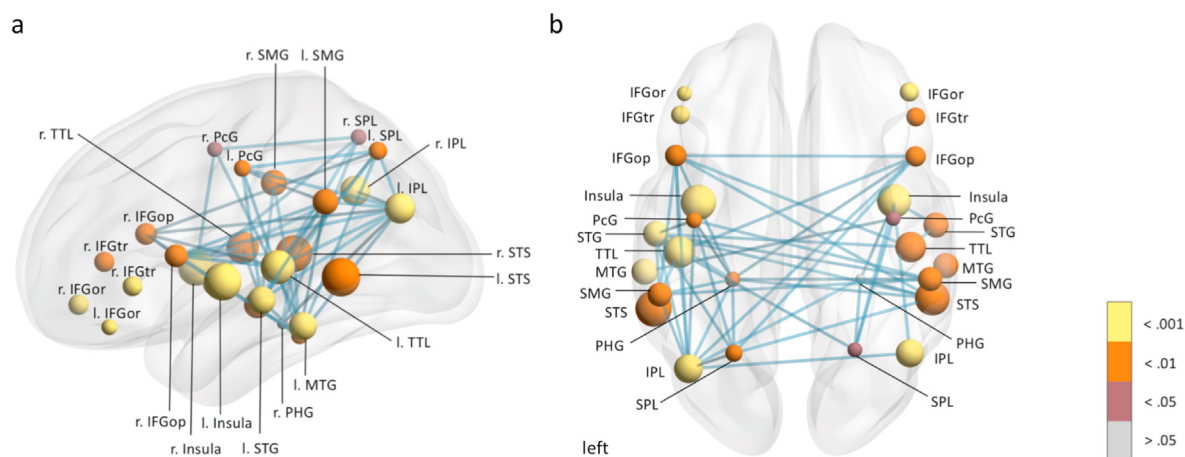


**Fig. 1** – Praxis network for TULIA total. The network (a left view, b dorsal view) consists of 13 bilateral ROIs with 169 connecting edges important for gesture production. Local efficiency values are represented by nodes and the edge values by lines. The statistical values derive from the prediction of gesture production by local efficiency and edge connectivity across groups. Only edges  $p < .0005$  (uncorrected) are depicted in the figure for a clearer presentation. The color of the nodes represents the  $p$ -value (FDR-corrected), whereas the size corresponds to the averaged local efficiency in healthy controls. The abbreviations are as follows: IFGop: pars opercularis of the IFG; IFGor: pars orbitalis of the IFG; IFGtr: pars triangularis of the IFG; PcG: precentral gyrus; SPL: superior parietal lobe; SMG: supramarginal gyrus; IPL: inferior parietal lobe; TTL: transverse temporal lobe; STG: superior temporal gyrus; STS: banks of superior temporal sulcus; PHG: parahippocampal gyrus; MTG: middle temporal gyrus. The brain network was visualized using the BrainNet Viewer software (<http://www.nitrc.org/projects/bnv/>) (Xia et al., 2013). A video of this figure is provided in the electronic version.

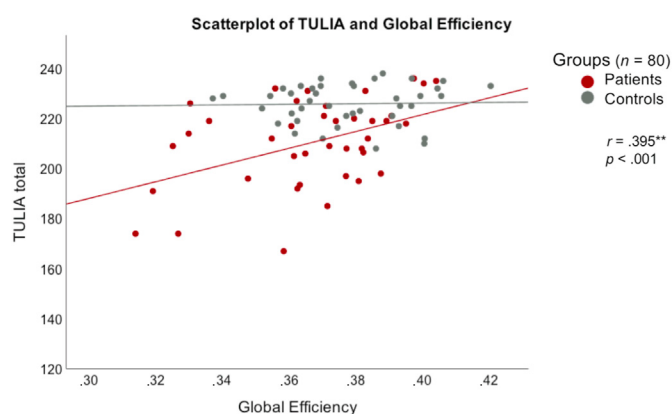


**Fig. 2** – Scatter plot of TULIA total score and global efficiency of the praxis network for patients with schizophrenia and healthy controls and least squares linear regression line (solid black line).

#### 4. Discussion

We aimed to investigate whether structural network organization and structural integrity of connections predict gesture production in healthy subjects and schizophrenia patients. We detected an association of gesture production with network attributes and specific connections within the praxis network. Thus, global and local efficiency and most of the intra- and interhemispheric connections within the praxis network were related to gesture production across groups. Global efficiency of the praxis network further predicted gesture production in the patient group. Local efficiency of

many ROIs and connections of interest were associated with gesture production in patients at trend-level. Furthermore, specifically imitation performance correlated with local efficiency of key regions and also structural integrity of selected tracts in patients. In contrast, there were no significant or trend-level associations of gesture production with network attributes in controls. Thus, we could only partly confirm the hypothesis, that local efficiency of key regions is associated with gesture performance, as it was not associated in the group of healthy controls. In patients, the association between performance and local efficiency of single key ROIs appears to be more pronounced for fundamental gesture skills, i.e., imitation. We conclude, that gesture production is associated

**Table 2 – Prediction of gesture production (TULIA total score) by global and local efficiency measures, across both groups and for each group separately.**

Structural connectivity measure	All subjects	Patients	Controls
Global efficiency ( <i>p</i> )	.001 <sup>a</sup>	.025 <sup>a</sup>	.779
Local efficiency ( <i>p</i> )			
Pars opercularis of IFG L	.002 <sup>a</sup>	.075	.570
Pars orbitalis of IFG L	.001 <sup>a</sup>	.005	.480
Pars triangularis of IFG L	.001 <sup>a</sup>	.009	.785
Precentral gyrus L	.002 <sup>a</sup>	.024	.846
Insula L	.001 <sup>a</sup>	.039	.785
Superior parietal lobe L	.008 <sup>a</sup>	.075	.534
Supramarginal gyrus L	.003 <sup>a</sup>	.064	.888
Inferior parietal lobe L	.001 <sup>a</sup>	.048	.495
Transverse temporal lobe L	.001 <sup>a</sup>	.021	.931
Superior temporal gyrus L	.001 <sup>a</sup>	.012	.770
Banks of STS L	.001 <sup>a</sup>	.017	.965
Parahippocampal gyrus L	.009 <sup>a</sup>	.063	.241
Middle temporal gyrus L	.001 <sup>a</sup>	.026	.874
Pars opercularis of IFG R	.003 <sup>a</sup>	.029	.883
Pars orbitalis of IFG R	.001 <sup>a</sup>	.037	.612
Pars triangularis of IFG R	.005 <sup>a</sup>	.093	.794
Precentral gyrus R	.013 <sup>a</sup>	.048	.639
Insula R	.001 <sup>a</sup>	.020	.934
Superior parietal lobe R	.013 <sup>a</sup>	.176	.160
Supramarginal gyrus R	.002 <sup>a</sup>	.030	.775
Inferior parietal lobe R	.001 <sup>a</sup>	.022	.301
Transverse temporal lobe R	.001 <sup>a</sup>	.027	.978
Superior temporal gyrus R	.002 <sup>a</sup>	.041	.955
Banks of STS R	.001 <sup>a</sup>	.050	.658
Parahippocampal gyrus R	.102	.194	.587
Middle temporal gyrus R	.005 <sup>a</sup>	.121	.814

<sup>a</sup> Survives FDR correction.

**Table 3 – Prediction of gesture production (TULIA total score) by structural integrity of selected connections/tracts across both groups and for each group separately.**

Connectivity/Tract of interest ( <i>p</i> )	All subjects	Patients	Controls
Connection between bilateral IFG	.001 <sup>a</sup>	.061	.413
Connection between bilateral IPL	.018 <sup>a</sup>	.106	.198
Connection between the IFG L and IPL L	.018 <sup>a</sup>	.044	.312
Uncinate fascicle L	.002 <sup>a</sup>	.113	.857
Superior longitudinal fascicle 3 L	.007 <sup>a</sup>	.038	.235
Arcuate fascicle L	.001 <sup>a</sup>	.012	.396
Fronto-parietal connection L	.007 <sup>a</sup>	.037	.539
Fronto-temporal connection L	.143	.522	.598
Connection between the IFG R and IPL R	.007 <sup>a</sup>	.133	.087
Uncinate fascicle R	.015 <sup>a</sup>	.338	.856
Superior longitudinal fascicle 3 R	.007 <sup>a</sup>	.183	.155
Arcuate fascicle R	.032 <sup>a</sup>	.279	.201
Fronto-parietal connection R	.029 <sup>a</sup>	.579	.055
Fronto-temporal connection R	.001 <sup>a</sup>	.010	.490

<sup>a</sup> Survives FDR correction.

with global and local efficiency and with specific connections of the praxis network. Our results indicate that especially subjects with gesture deficits have alterations in the organization of the praxis network. Gesture production is not related

to one single brain region, but instead is associated with a highly-connected bilateral network of various frontal, parietal and temporal regions.

A number of fMRI studies in healthy subjects revealed the importance of the praxis network for the planning and execution of different gesture types. The execution of tool use in healthy subjects depends on the parietal lobe, temporal areas, the dorsal and ventral premotor cortex and the inferior frontal areas (Hermesdorfer et al., 2007; Johnson-Frey et al., 2005). Planning of tool use involves the same regions as the execution of it, with the exception of the dorsolateral prefrontal cortex, which is important for planning (Johnson-Frey et al., 2005). In addition, planning of tool use pantomime and intransitive gestures depend again on similar regions of the praxis network, including the IPS, SMG, SPL and premotor areas (Kroliczak & Frey, 2009).

Our results further support the idea that also the structural integrity of selected connections and tracts of the praxis network are important for gesture production. Thus, we not only revealed an association of global network efficiency and gesture production, but also of local efficiency of all ROIs of the praxis network (except the right parahippocampal gyrus). In addition, we detected associations of all selected connections/tracts of the praxis network with gesture production (except for the left fronto-temporal connection). These connections include the interhemispheric connections between the bilateral IFG and IPL, intrahemispheric fronto-parietal and fronto-temporal connections, the SLF III, arcuate and uncinate fascicle.

Two structures of the praxis network are particularly important in gesture production, the IFG and the IPL. The pars opercularis of the IFG has been linked to language production, as it is part of Broca's area, and to motor functions, as it combines sensory stimuli with hand actions (Binkofski & Buccino, 2004). Hence, lesions in this area have been related to simultaneous aphasia and apraxia, emphasizing the role of the IFG as an intersection between language and praxis (Weiss et al., 2016). The IPL integrates motor information with visuospatial and cognitive inputs (Fogassi & Luppino, 2005; Gottlieb, 2007). Therefore, the IPL processes motor acts, such as grasping (Fogassi & Luppino, 2005), and cognitive motor functions, including the comprehension of intention (Fogassi & Luppino, 2005) and observation of tool use gestures (Buccino et al., 2001).

The importance of these two key regions is strongly supported by studies in healthy subjects and in patients with apraxia. In healthy subjects, fMRI studies revealed activations in the IFG and IPL for the planning and execution of tool use and planning of intransitive gestures (Fridman et al., 2006; Johnson-Frey et al., 2005; Vry et al., 2015). In line with these results, lesion studies emphasize the role of the IFG in the pantomime of tool use and imitation of meaningless finger gestures (Goldenberg et al., 2007; Goldenberg & Karnath, 2006). In addition, the parietal lobe has been suggested to be involved in actual tool use and imitation of meaningless gestures (Goldenberg, 2009), but not in pantomime of tool use (Goldenberg et al., 2007). However, there is also evidence that pantomime of tool use is linked to IPL lesions (Buxbaum et al., 2014; Hoeren et al., 2014; Manuel et al., 2013; Weiss et al., 2016). Furthermore, one study revealed an association of white matter integrity between the IFG and IPL and tool use performance in brain-damaged patients (Bi et al., 2015).



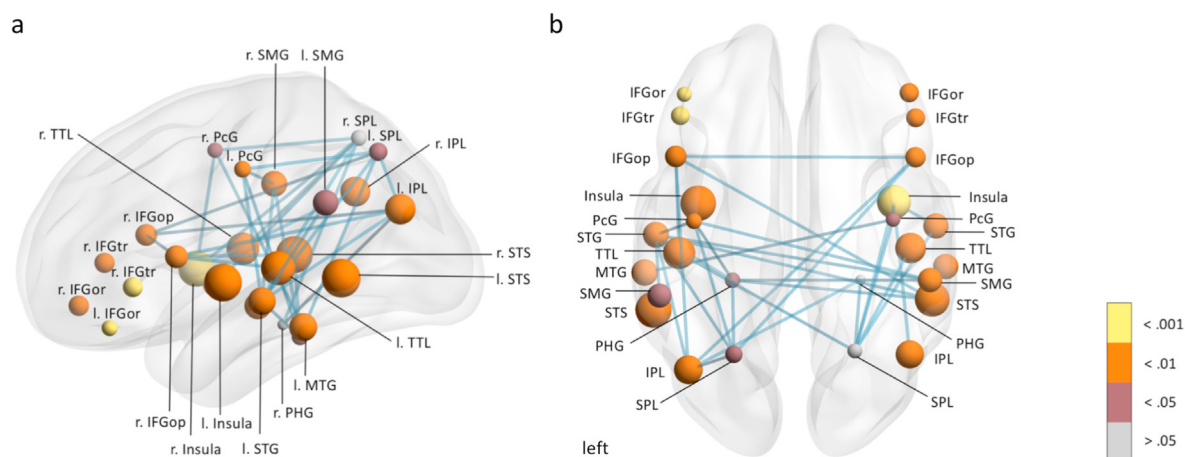


**Fig. 3 – Praxis networks for pantomime.** The network (a left view, b dorsal view) consists of 13 bilateral ROIs with 169 connecting edges important for gesture production. Local efficiency values are represented by nodes and the edge values by lines. The statistical values derive from the prediction of pantomime and imitation by local efficiency and edge connectivity across groups. Only edges  $p < .0005$  (uncorrected) are depicted in the figure for a clearer presentation. The color of the nodes represents the  $p$ -value (FDR-corrected), whereas the size corresponds to the averaged local efficiency in healthy controls. The abbreviations are as follows: IFGop: pars opercularis of the IFG; IFGor: pars orbitalis of the IFG; IFGtr: pars triangularis of the IFG; PcG: precentral gyrus; SPL: superior parietal lobe; SMG: supramarginal gyrus; IPL: inferior parietal lobe; TTL: transverse temporal lobe; STG: superior temporal gyrus; STS: banks of superior temporal sulcus; PHG: parahippocampal gyrus; MTG: middle temporal gyrus. The brain network was visualized using the BrainNet Viewer software (<http://www.nitrc.org/projects/bnv/>) (Xia et al., 2013). A video of this figure is provided in the electronic version.

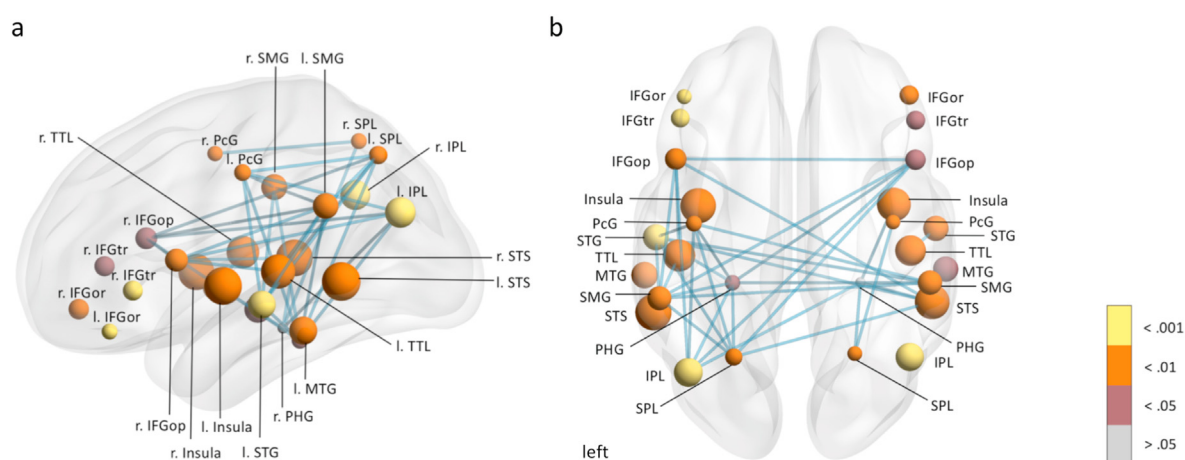


**Fig. 4 – Praxis networks for imitation.** The network (a left view, b dorsal view) consists of 13 bilateral ROIs with 169 connecting edges important for gesture production. Local efficiency values are represented by nodes and the edge values by lines. The statistical values derive from the prediction of pantomime and imitation by local efficiency and edge connectivity across groups. Only edges  $p < .0005$  (uncorrected) are depicted in the figure for a clearer presentation. The color of the nodes represents the  $p$ -value (FDR-corrected), whereas the size corresponds to the averaged local efficiency in healthy controls. The abbreviations are as follows: IFGop: pars opercularis of the IFG; IFGor: pars orbitalis of the IFG; IFGtr: pars triangularis of the IFG; PcG: precentral gyrus; SPL: superior parietal lobe; SMG: supramarginal gyrus; IPL: inferior parietal lobe; TTL: transverse temporal lobe; STG: superior temporal gyrus; STS: banks of superior temporal sulcus; PHG: parahippocampal gyrus; MTG: middle temporal gyrus. The brain network was visualized using the BrainNet Viewer software (<http://www.nitrc.org/projects/bnv/>) (Xia et al., 2013). A video of this figure is provided in the electronic version.

In line with these results, our findings indicate that also the connections between the IFG and the IPL are significantly involved in gesturing. We found a strong association of these two core regions with gesture production. This was not only

evident in connections between the IFG and the IPL, but also in interhemispheric connections between the bilateral IFG and bilateral IPL. Furthermore, the local efficiency of the bilateral IFG and IPL significantly predicted gesture production



indicating that these ROIs are highly connected and constitute central regions of the praxis network.

In healthy subjects, two studies have investigated structural connections implicated in gesture production. Our results corroborate and extend the findings of these pilot studies in a large sample. The first study identified four structural pathways connecting important areas for tool use (Ramayya et al., 2010). However, this study did not investigate the association of these connections with a behavioral measurement. Despite the fact that we used slightly different defined ROIs, we confirmed the importance of the four structural connections in gesture production. More precisely, our edge-level analyses revealed that gesture production is associated with the connection between the opercular part of the IFG and the IPL. Furthermore, gesture production is also associated with the connectivity between the MTG and the IPL. Thus, our findings support the importance of these four connections in gesture production by linking them to a behavioral measurement of gesturing. The second study indicates that imitation of meaningless gestures and pantomime of tool use depend on the dorso-dorsal stream for action semantics, and that only pantomime depends additionally on the ventral stream for specific conceptual operations (Vry et al., 2015). In line with this study, we revealed that the connectivity of the dorsal stream, including the bilateral SLF III and AF, predicted gesture performance across groups. The ventral pathway is described as connecting the pars triangularis of the IFG with parietal and temporal regions via the extreme capsule (Vry et al., 2015). In our study, we were interested in a fronto-temporal and fronto-parietal connection. Whereas the former connects the pars triangularis of the IFG with the banks of the STS and superior, middle and inferior temporal gyrus, the latter connects the same frontal region with the IPL. As only the fronto-temporal connection is to some extent congruent with the ventral pathway as defined by Vry et al. (2015), our results only partly support the role of this pathway. Nevertheless, our results are in line with the preliminary findings about the role of structural connectivity for gesture production.

A major part of the association between gesture production and connectivity of the praxis network results from subjects with gesture deficits. Schizophrenia is characterized by altered network connectivity and topological organization, including altered global network communication and disrupted structural hub connectivity (van den Heuvel & Fornito, 2014). Our findings revealed a link of a disturbed network with behavioral associations in a continuum from healthy subjects to a patient group, which is characterized by microstructural WM abnormalities. Global efficiency of the praxis network significantly predicted gesture production in patients with schizophrenia. Local efficiency and specific structural connections showed trend-level associations. In contrast, healthy subjects revealed no association between the connectivity of the praxis network and gesture production. This suggests that gesture impairments only occur if the organization of the praxis network is critically altered.

Our sample of schizophrenia patients is characterized by a large variance in gesture production, including patients with intact and disturbed gesture production. In schizophrenia patients, deficits in imitation are less frequently observed than deficits in pantomime and are consequently particularly

evident in patients with severe gesture deficits (Walther et al., 2013, 2015). Therefore, these patients are expected to show also pronounced structural dysconnectivity of the praxis network (Walther & Mittal, 2016). Indeed, when we ran the same analysis separate for each gesture domain, imitation of gesture was further predicted by the local efficiency of many ROIs, encompassing the IFG, SPL, and IPL (including SMG), temporal regions (STG and MTG) and different specific connections between those ROIs, such as the AF, SLF, fronto-temporal and fronto-parietal connections. In line with these results, our earlier work demonstrated GM reductions and cortical thinning of the praxis network in schizophrenia patients with gesture deficits as well as aberrant activity in the dorsolateral prefrontal cortex and inferior parietal lobe (Stegmayer et al., 2016, 2017; Viher et al., 2018). Furthermore, repetitive transcranial magnetic stimulation on IFG and IPL improved gesture production in patients (Walther et al., 2020).

Some limitations of our study require discussion. First, we cannot exclude a possible effect of medication on our findings. However, the effect of medication on WM remains controversial and many studies did not show an effect of antipsychotic medication on WM structure in schizophrenia (Hajjma et al., 2013; Liu et al., 2013; Peters et al., 2010). As our sample included healthy subjects and patients, the statistical analyses did not allow to correct for any possible medication effect. Still, a separate analysis in patients with schizophrenia failed to detect an association between medication dosages and global efficiency in the praxis network. We further tested for associations between the severity of the PANSS total score and duration of illness with global efficiency in patients with schizophrenia. The analysis for the PANSS total score failed to detect an association ( $r = .174, p > .05$ ). In contrast, the association between duration of illness and global efficiency was significant ( $r = -.536, p < .05$ ). However, because duration of illness and age are also significantly correlated (and because we already control for age) we did not additionally control for duration of illness. In fact, the correlation between duration of illness and global efficiency is not significant if we correct it for age ( $r = -.098, p > .05$ ).

Second, different demographic factors influence WM microstructure. For example, age-related reductions in FA have frequently been reported, predominantly in frontal brain areas (Gunning-Dixon et al., 2009; Phillips et al., 2013; Salat et al., 2005). In addition to age, sex is also related to WM changes, depending on the interested brain region (Kanaan et al., 2012, 2014; Menzler et al., 2011; Phillips et al., 2013). Therefore, we included both variables in addition to TIV as covariates into all of our analyses. Third, we selected out of an atlas 13 predefined bilateral ROIs (Desikan et al., 2006) that are important in gesturing. In addition, we selected some specific connections of interest based on the literature. These arbitrary selections might have missed other brain areas or connections that are possibly involved in gesturing. Fourth, graph theory includes several measures that characterize the network. As it is not yet elucidated which of the measures are most appropriate to analyze brain networks (Bullmore & Sporns, 2009), we chose, due to our research question, global and local efficiency and some specific connections of interest. However, other measurements such as the shortest

path length, clustering coefficient or connection density could also be of interest.

Taken together, the present study explored whether the structural connectivity of the praxis network is related to gesture production. Our results indicate that a high global and local efficiency of the praxis network is associated with intact production of gestures. Defective gesturing is linked to a less efficient praxis network, which is underpinned by the association of global network efficiency and gesture production in patients with schizophrenia. Reduced structural connectivity between key regions of the praxis network, including intra- and interhemispheric connections between the IFG and the IPL, is further related to impaired gesture production across groups. In addition, the SLF, AF, UF and specific fronto-temporal and fronto-parietal connections are involved in gesturing. In sum, our results revealed that structural alterations of the praxis network are associated with gesture production deficits. These findings contribute to the understanding of the neural correlates in gesture production. However, how these regions are functionally connected and how dynamic each region of the network acts, remains to be investigated by future studies.

---

### Credit author statement

P.V.V. analyzed the data and wrote the manuscript. A.A., P.S., M.K., N.M., S.K., A.F. and R.W. were involved in data analysis and provided methodological support. K.S. was involved in data collection. S.B., A.F., and S.W. designed the study and acquired funding. A.A., A.F. K.S., T.V., R.M., S.B., and W.S. edited the manuscript. S.W. wrote the protocol, was involved in writing the manuscript, and supervised the study. All authors approved to the final manuscript.

---

### Funding

This work was supported by the Bangerter-Rhyner Foundation (to Sebastian Walther), the Swiss National Science Foundation (SNF grant 152619/1 to Sebastian Walther, Andrea Federspiel, and Stephan Bohlhalter and SNF grant 173880 for Ahmed Abdulkadir) and a NARSAD Young Investigator Award from the Brain and Behavior Research Foundation (grant 22591 to Peter Savadjiev).

---

### Declaration of competing interest

All authors declare that they have no conflict of interest.

---

### Supplementary data

Supplementary data to this article can be found online at <https://doi.org/10.1016/j.cortex.2020.05.023>.

---

### REFERENCES

- Andreasen, N. C., Flaum, M., & Arndt, S. (1992). The Comprehensive Assessment of Symptoms and History (CASH). An instrument for assessing diagnosis and psychopathology. *Archives of General Psychiatry*, 49, 615–623.
- Bi, Y., Han, Z., Zhong, S., Ma, Y., Gong, G., Huang, R., Song, L., Fang, Y., He, Y., & Caramazza, A. (2015). The white matter structural network underlying human tool use and tool understanding. *The Journal of Neuroscience*, 35, 6822–6835.
- Binkofski, F., & Buccino, G. (2004). Motor functions of the Broca's region. *Brain and Language*, 89, 362–369.
- Binkofski, F., & Buxbaum, L. J. (2013). Two action systems in the human brain. *Brain and Language*, 127, 222–229.
- Bohlhalter, S., Hattori, N., Wheaton, L., Fridman, E., Shamim, E. A., Garraux, G., & Hallett, M. (2009). Gesture subtype-dependent left lateralization of praxis planning: An event-related fMRI study. *Cerebral Cortex*, 19, 1256–1262.
- Buccino, G., Binkofski, F., Fink, G. R., Fadiga, L., Fogassi, L., Gallese, V., Seitz, R. J., Zilles, K., Rizzolatti, G., & Freund, H. J. (2001). Action observation activates premotor and parietal areas in a somatotopic manner: An fMRI study. *The European Journal of Neuroscience*, 13, 400–404.
- Bullmore, E., & Sporns, O. (2009). Complex brain networks: Graph theoretical analysis of structural and functional systems. *Nature Reviews. Neuroscience*, 10, 186–198.
- Buxbaum, L. J., Shapiro, A. D., & Coslett, H. B. (2014). Critical brain regions for tool-related and imitative actions: A componential analysis. *Brain*, 137, 1971–1985.
- Catani, M., Howard, R. J., Pajevic, S., & Jones, D. K. (2002). Virtual in vivo interactive dissection of white matter fasciculi in the human brain. *Neuroimage*, 17, 77–94.
- Dale, A. M., Fischl, B., & Sereno, M. I. (1999). Cortical surface-based analysis. I. Segmentation and surface reconstruction. *Neuroimage*, 9, 179–194.
- Deichmann, R., Schwarzbauer, C., & Turner, R. (2004). Optimisation of the 3D MDEFT sequence for anatomical brain imaging: Technical implications at 1.5 and 3 T. *Neuroimage*, 21, 757–767.
- Del Re, E. C., Gao, Y., Eckbo, R., Petryshen, T. L., Blokland, G. A., Seidman, L. J., Konishi, J., Goldstein, J. M., McCarley, R. W., Shenton, M. E., & Bouix, S. (2016). A new MRI masking technique based on multi-atlas brain segmentation in controls and schizophrenia: A rapid and viable alternative to manual masking. *Journal of Neuroimaging*, 26, 28–36.
- Dela Haije, T., Savadjiev, P., Fuster, A., Schultz, R. T., Verma, R., Florack, L., & Westin, C. F. (2019). Structural connectivity analysis using finlser geometry. *SIAM Journal on Imaging Sciences*, 12, 551–575.
- Desikan, R. S., Segonne, F., Fischl, B., Quinn, B. T., Dickerson, B. C., Blacker, D., Buckner, R. L., Dale, A. M., Maguire, R. P., Hyman, B. T., Albert, M. S., & Killiany, R. J. (2006). An automated labeling system for subdividing the human cerebral cortex on MRI scans into gyral based regions of interest. *Neuroimage*, 31, 968–980.
- Duffau, H., Gatignol, P., Mandonnet, E., Peruzzi, P., Tzourio-Mazoyer, N., & Capelle, L. (2005). New insights into the anatomo-functional connectivity of the semantic system: A study using cortico-subcortical electrostimulations. *Brain*, 128, 797–810.
- Duffau, H., Peggy Gatignol, S. T., Mandonnet, E., Capelle, L., & Taillandier, L. (2008). Intraoperative subcortical stimulation mapping of language pathways in a consecutive series of 115 patients with Grade II glioma in the left dominant hemisphere. *Journal of Neurosurgery*, 109, 461–471.
- Faul, F., Erdfelder, E., Buchner, A., & Lang, A. G. (2009). Statistical power analyses using G\*power 3.1: Tests for correlation and regression analyses. *Behavior Research Methods*, 41, 1149–1160.
- Faul, F., Erdfelder, E., Lang, A. G., & Buchner, A. (2007). G\*Power 3: A flexible statistical power analysis program for the social, behavioral, and biomedical sciences. *Behavior Research Methods*, 39, 175–191.
- Fischl, B. (2012). FreeSurfer. *Neuroimage*, 62, 774–781.

- Fischl, B., Sereno, M. I., & Dale, A. M. (1999). Cortical surface-based analysis. II: Inflation, flattening, and a surface-based coordinate system. *Neuroimage*, 9, 195–207.
- Fogassi, L., & Luppino, G. (2005). Motor functions of the parietal lobe. *Current Opinion in Neurobiology*, 15, 626–631.
- Fridman, E. A., Immisch, I., Hanakawa, T., Bohlhalter, S., Waldvogel, D., Kansaku, K., Wheaton, L., Wu, T., & Hallett, M. (2006). The role of the dorsal stream for gesture production. *Neuroimage*, 29, 417–428.
- Geschwind, N. (1965). Disconnexion syndromes in animals and man. II. *Brain*, 88, 585–644.
- Goldenberg, G. (2009). Apraxia and the parietal lobes. *Neuropsychologia*, 47, 1449–1459.
- Goldenberg, G., & Hagmann, S. (1998). Tool use and mechanical problem solving in apraxia. *Neuropsychologia*, 36, 581–589.
- Goldenberg, G., Hermsdorfer, J., Glindemann, R., Rorden, C., & Karnath, H. O. (2007). Pantomime of tool use depends on integrity of left inferior frontal cortex. *Cerebral Cortex*, 17, 2769–2776.
- Goldenberg, G., & Karnath, H. O. (2006). The neural basis of imitation is body part specific. *The Journal of Neuroscience*, 26, 6282–6287.
- Goldenberg, G., & Spatt, J. (2009). The neural basis of tool use. *Brain*, 132, 1645–1655.
- Goldin-Meadow, S., & Alibali, M. W. (2013). Gesture's role in speaking, learning, and creating language. *Annual Review of Psychology*, 64, 257–283.
- Gottlieb, J. (2007). From thought to action: The parietal cortex as a bridge between perception, action, and cognition. *Neuron*, 53, 9–16.
- Gunning-Dixon, F. M., Brickman, A. M., Cheng, J. C., & Alexopoulos, G. S. (2009). Aging of cerebral white matter: A review of MRI findings. *International Journal of Geriatric Psychiatry*, 24, 109–117.
- Haaland, K. Y., Harrington, D. L., & Knight, R. T. (2000). Neural representations of skilled movement. *Brain*, 123(Pt 11), 2306–2313.
- Haijma, S. V., Van Haren, N., Cahn, W., Koolschijn, P. C., Hulshoff Pol, H. E., & Kahn, R. S. (2013). Brain volumes in schizophrenia: A meta-analysis in over 18 000 subjects. *Schizophrenia Bulletin*, 39, 1129–1138.
- Hermsdorfer, J., Li, Y., Randerath, J., Roby-Brami, A., & Goldenberg, G. (2013). Tool use kinematics across different modes of execution. Implications for action representation and apraxia. *Cortex*, 49, 184–199.
- Hermsdorfer, J., Terlinden, G., Muhlau, M., Goldenberg, G., & Wohlschlagel, A. M. (2007). Neural representations of pantomimed and actual tool use: Evidence from an event-related fMRI study. *Neuroimage*, 36(Suppl 2), T109–T118.
- Hoeren, M., Kummerer, D., Bormann, T., Beume, L., Ludwig, V. M., Vry, M. S., Mader, I., Rijntjes, M., Kaller, C. P., & Weiller, C. (2014). Neural bases of imitation and pantomime in acute stroke patients: Distinct streams for praxis. *Brain*, 137, 2796–2810.
- Johnson-Frey, S. H., Newman-Norlund, R., & Grafton, S. T. (2005). A distributed left hemisphere network active during planning of everyday tool use skills. *Cerebral Cortex*, 15, 681–695.
- Kanaan, R. A., Allin, M., Picchioni, M., Barker, G. J., Daly, E., Shergill, S. S., Woolley, J., & McGuire, P. K. (2012). Gender differences in white matter microstructure. *Plos One*, 7, e38272.
- Kanaan, R. A., Chaddock, C., Allin, M., Picchioni, M. M., Daly, E., Shergill, S. S., & McGuire, P. K. (2014). Gender influence on white matter microstructure: A tract-based spatial statistics analysis. *Plos One*, 9, e91109.
- Kay, S. R., Fiszbein, A., & Opler, L. A. (1987). The positive and negative syndrome scale (PANSS) for schizophrenia. *Schizophrenia Bulletin*, 13, 261–276.
- Kroliczak, G., & Frey, S. H. (2009). A common network in the left cerebral hemisphere represents planning of tool use pantomimes and familiar intransitive gestures at the hand-independent level. *Cerebral Cortex*, 19, 2396–2410.
- Latora, V., & Marchiori, M. (2001). Efficient behavior of small-world networks. *Physical Review Letters*, 87, 198701.
- Lavelle, M., Healey, P. G., & McCabe, R. (2013). Is nonverbal communication disrupted in interactions involving patients with schizophrenia? *Schizophrenia Bulletin*, 39, 1150–1158.
- Liu, X., Lai, Y., Wang, X., Hao, C., Chen, L., Zhou, Z., Yu, X., & Hong, N. (2013). Reduced white matter integrity and cognitive deficit in never-medicated chronic schizophrenia: A diffusion tensor study using TBSS. *Behavioural Brain Research*, 252, 157–163.
- Makris, N., Kennedy, D. N., McInerney, S., Sorensen, A. G., Wang, R., Caviness, V. S., Jr., & Pandya, D. N. (2005). Segmentation of subcomponents within the superior longitudinal fascicle in humans: A quantitative, in vivo, DT-MRI study. *Cerebral Cortex*, 15, 854–869.
- Makris, N., & Pandya, D. N. (2009). The extreme capsule in humans and rethinking of the language circuitry. *Brain Structure & Function*, 213, 343–358.
- Malcolm, J. G., Shenton, M. E., & Rathi, Y. (2010). Filtered multitensor tractography. *IEEE Transactions on Medical Imaging*, 29, 1664–1675.
- Manuel, A. L., Radman, N., Mesot, D., Chouiter, L., Clarke, S., Annoni, J. M., & Spierer, L. (2013). Inter- and intrahemispheric dissociations in ideomotor apraxia: A large-scale lesion-symptom mapping study in subacute brain-damaged patients. *Cerebral Cortex*, 23, 2781–2789.
- Mengotti, P., Corradi-Dell'Acqua, C., Negri, G. A., Ukmar, M., Pesavento, V., & Rumiati, R. I. (2013). Selective imitation impairments differentially interact with language processing. *Brain*, 136, 2602–2618.
- Menzler, K., Belke, M., Wehrmann, E., Krakow, K., Lengler, U., Jansen, A., Hamer, H. M., Oertel, W. H., Rosenow, F., & Knake, S. (2011). Men and women are different: Diffusion tensor imaging reveals sexual dimorphism in the microstructure of the thalamus, corpus callosum and cingulum. *Neuroimage*, 54, 2557–2562.
- Millman, Z. B., Goss, J., Schiffman, J., Mejias, J., Gupta, T., & Mittal, V. A. (2014). Mismatch and lexical retrieval gestures are associated with visual information processing, verbal production, and symptomatology in youth at high risk for psychosis. *Schizophrenia Research*, 158, 64–68.
- Nichols, T., & Hayasaka, S. (2003). Controlling the familywise error rate in functional neuroimaging: A comparative review. *Statistical Methods in Medical Research*, 12, 419–446.
- Oldfield, R. C. (1971). The assessment and analysis of handedness: The Edinburgh inventory. *Neuropsychologia*, 9, 97–113.
- Peters, B. D., Blaas, J., & de Haan, L. (2010). Diffusion tensor imaging in the early phase of schizophrenia: What have we learned? *Journal of Psychiatric Research*, 44, 993–1004.
- Petrides, M., & Pandya, D. N. (1988). Association fiber pathways to the frontal cortex from the superior temporal region in the rhesus monkey. *Journal of Comparative Neurology*, 273, 52–66.
- Phillips, O. R., Clark, K. A., Luders, E., Azhir, R., Joshi, S. H., Woods, R. P., Mazziotta, J. C., Toga, A. W., & Narr, K. L. (2013). Superficial white matter: Effects of age, sex, and hemisphere. *Brain Connectivity*, 3, 146–159.
- Pouw, W. T., de Nooijer, J. A., van Gog, T., Zwaan, R. A., & Paas, F. (2014). Toward a more embedded/extended perspective on the cognitive function of gestures. *Frontiers in Psychology*, 5, 359.
- Ramayya, A. G., Glasser, M. F., & Rilling, J. K. (2010). A DTI investigation of neural substrates supporting tool use. *Cerebral Cortex*, 20, 507–516.
- Randerath, J., Goldenberg, G., Spijkers, W., Li, Y., & Hermsdorfer, J. (2010). Different left brain regions are essential for grasping a



- tool compared with its subsequent use. *Neuroimage*, 53, 171–180.
- Rilling, J. K., Glasser, M. F., Preuss, T. M., Ma, X., Zhao, T., Hu, X., & Behrens, T. E. (2008). The evolution of the arcuate fasciculus revealed with comparative DTI. *Nature Neuroscience*, 11, 426–428.
- Rubinov, M., & Sporns, O. (2010). Complex network measures of brain connectivity: Uses and interpretations. *Neuroimage*, 52, 1059–1069.
- Salat, D. H., Tuch, D. S., Greve, D. N., van der Kouwe, A. J., Hevelone, N. D., Zaleta, A. K., Rosen, B. R., Fischl, B., Corkin, S., Rosas, H. D., & Dale, A. M. (2005). Age-related alterations in white matter microstructure measured by diffusion tensor imaging. *Neurobiology of Aging*, 26, 1215–1227.
- Sheehan, D. V., Lecrubier, Y., Sheehan, K. H., Amorim, P., Janavs, J., Weiller, E., Hergueta, T., Baker, R., & Dunbar, G. C. (1998). The mini-international neuropsychiatric Interview (M.I.N.I.): The development and validation of a structured diagnostic psychiatric interview for DSM-IV and ICD-10. *Journal of Clinical Psychiatry*, 59(Suppl 20), 22–33. quiz 34–57.
- Sporns, O. (2013). Structure and function of complex brain networks. *Dialogues in Clinical Neuroscience*, 15, 247–262.
- Stegmayer, K., Bohlhalter, S., Vanbellingen, T., Federspiel, A., Moor, J., Wiest, R., Muri, R., Strik, W., & Walther, S. (2016). Structural brain correlates of defective gesture performance in schizophrenia. *Cortex*, 78, 125–137.
- Stegmayer, K., Bohlhalter, S., Vanbellingen, T., Federspiel, A., Wiest, R., Muri, R. M., ... Walther, S. (2017). Limbic interference during social action planning in schizophrenia. *Schizophrenia Bulletin*, 44, 359–368.
- van den Heuvel, M. P., & Fornito, A. (2014). Brain networks in schizophrenia. *Neuropsychology Review*, 24, 32–48.
- van den Heuvel, M. P., Sporns, O., Collin, G., Scheewe, T., Mandl, R. C., Cahn, W., Goni, J., Hulshoff Pol, H. E., & Kahn, R. S. (2013). Abnormal rich club organization and functional brain dynamics in schizophrenia. *JAMA Psychiatry*, 70, 783–792.
- Vanbellingen, T., Kersten, B., Van Hemelrijk, B., Van de Winckel, A., Bertschi, M., Muri, R., De Weerd, W., & Bohlhalter, S. (2010). Comprehensive assessment of gesture production: A new test of upper limb apraxia (TULIA). *European Journal of Neurology*, 17, 59–66.
- Viher, P. V., Stegmayer, K., Kubicki, M., Karmacharya, S., Lyall, A. E., Federspiel, A., Vanbellingen, T., Bohlhalter, S., Wiest, R., Strik, W., & Walther, S. (2018). The cortical signature of impaired gesturing: Findings from schizophrenia. *Neuroimage Clinics*, 17, 213–221.
- Vry, M. S., Tritschler, L. C., Hamzei, F., Rijntjes, M., Kaller, C. P., Hoeren, M., Umarova, R., Glauche, V., Hermsdoerfer, J., Goldenberg, G., Hennig, J., & Weiller, C. (2015). The ventral fiber pathway for pantomime of object use. *Neuroimage*, 106, 252–263.
- Walther, S., Kunz, M., Muller, M., Zurcher, C., Vladimirova, I., Bachofner, H., ... Viher, P. V. (2020). Single session transcranial magnetic stimulation ameliorates hand gesture deficits in schizophrenia. *Schizophrenia Bulletin*, 46, 286–293.
- Walther, S., & Mittal, V. A. (2016). Why we should take a closer look at gestures. *Schizophrenia Bulletin*, 42, 259–261.
- Walther, S., Stegmayer, K., Sulzbacher, J., Vanbellingen, T., Muri, R., Strik, W., & Bohlhalter, S. (2015). Nonverbal social communication and gesture control in schizophrenia. *Schizophrenia Bulletin*, 41, 338–345.
- Walther, S., Vanbellingen, T., Muri, R., Strik, W., & Bohlhalter, S. (2013). Impaired gesture performance in schizophrenia: Particular vulnerability of meaningless pantomimes. *Neuropsychologia*, 51, 2674–2678.
- Wassermann, D., Makris, N., Rathi, Y., Shenton, M., Kikinis, R., Kubicki, M., & Westin, C. F. (2016). The white matter query language: A novel approach for describing human white matter anatomy. *Brain Structure & Function*, 221, 4705–4721.
- Weiss, P. H., Ubben, S. D., Kaesberg, S., Kalbe, E., Kessler, J., Liebig, T., & Fink, G. R. (2016). Where language meets meaningful action: A combined behavior and lesion analysis of aphasia and apraxia. *Brain Structure & Function*, 221, 563–576.
- Whitford, T. J., Kubicki, M., & Shenton, M. E. (2011). Diffusion tensor imaging, structural connectivity, and schizophrenia. *Schizophr Research Treatment*, 2011, 709523.
- Woods, S. W. (2003). Chlorpromazine equivalent doses for the newer atypical antipsychotics. *Journal of Clinical Psychiatry*, 64, 663–667.
- Xia, M., Wang, J., & He, Y. (2013). BrainNet viewer: A network visualization tool for human brain connectomics. *Plos One*, 8, e68910.